Published OnlineFirst December 20, 2011; DOI:10.1158/0008-5472.CAN-11-1620

Cancer Research

Immune Inhibitory Molecules LAG-3 and PD-1 Synergistically Regulate T-cell Function to Promote Tumoral Immune Escape

Seng-Ryong Woo, Meghan E. Turnis, Monica V. Goldberg, et al.

Cancer Res 2012;72:917-927. Published OnlineFirst December 20, 2011.

Updated Version Access the most recent version of this article at: doi:10.1158/0008-5472.CAN-11-1620

Supplementary Material Access the most recent supplemental material at: http://cancerres.aacrjournals.org/content/suppl/2011/12/19/0008-5472.CAN-11-1620.DC1.html

Cited Articles This article cites 50 articles, 25 of which you can access for free at: http://cancerres.aacrjournals.org/content/72/4/917.full.html#ref-list-1

Citing Articles This article has been cited by 1 HighWire-hosted articles. Access the articles at: http://cancerres.aacrjournals.org/content/72/4/917.full.html#related-urls

E-mail alerts Sign up to receive free email-alerts related to this article or journal.

Reprints and Subscriptions To order reprints of this article or to subscribe to the journal, contact the AACR Publications Department at pubs@aacr.org.

Permissions To request permission to re-use all or part of this article, contact the AACR Publications Department at permissions@aacr.org.

Downloaded from cancerres.aacrjournals.org on July 6, 2012
Copyright © 2012 American Association for Cancer Research

Published OnlineFirst December 20, 2011; DOI:10.1158/0008-5472.CAN-11-1620

Immune Inhibitory Molecules LAG-3 and PD-1 Synergistically Regulate T-cell Function to Promote Tumoral Immune Escape

Seng-Ryong Woo[1], Meghan E. Turnis[1], Monica V. Goldberg[4], Jaishree Bankoti[1], Mark Selby[8], Christopher J. Nirschl[4], Matthew L. Bettini[1], David M. Gravano[1], Peter Vogel[2], Chih Long Liu[9], Stephanie Tangsombatvisit[9], Joseph F. Grosso[4], George Netto[6], Matthew P. Smeltzer[3], Alcides Chaux[7], Paul J. Utz[9], Creg J. Workman[1], Drew M. Pardoll[5], Alan J. Korman[8], Charles G. Drake[4], and Dario A.A. Vignali[1]

Abstract

Inhibitory receptors on immune cells are pivotal regulators of immune escape in cancer. Among these inhibitory receptors, CTLA-4 (targeted clinically by ipilimumab) serves as a dominant off-switch while other receptors such as PD-1 and LAG-3 seem to serve more subtle rheostat functions. However, the extent of synergy and cooperative interactions between inhibitory pathways in cancer remain largely unexplored. Here, we reveal extensive coexpression of PD-1 and LAG-3 on tumor-infiltrating $CD4^+$ and $CD8^+$ T cells in three distinct transplantable tumors. Dual anti–LAG-3/anti–PD-1 antibody treatment cured most mice of established tumors that were largely resistant to single antibody treatment. Despite minimal immunopathologic sequelae in PD-1 and LAG-3 single knockout mice, dual knockout mice abrogated self-tolerance with resultant autoimmune infiltrates in multiple organs, leading to eventual lethality. However, $Lag3^{-/-}Pdcd1^{-/-}$ mice showed markedly increased survival from and clearance of multiple transplantable tumors. Together, these results define a strong synergy between the PD-1 and LAG-3 inhibitory pathways in tolerance to both self and tumor antigens. In addition, they argue strongly that dual blockade of these molecules represents a promising combinatorial strategy for cancer. *Cancer Res; 72(4); 917–27. ©2011 AACR.*

Introduction

T-cell–mediated antitumor immune responses are essential for effective deletion of primary tumor lesions and for protection against metastases (1). Although the immune system can detect and destroy malignant cells, tumors escape surveillance by a variety of cell intrinsic and extrinsic mechanisms (1–3). As with chronic viral infection (4), tumor antigen-specific $CD4^+$ and $CD8^+$ T cells display impaired effector function and an exhausted phenotype characterized by decreased production of proinflammatory cytokines and hyporesponsiveness to antigenic restimulation (5). This is mediated by cell extrinsic mechanisms, such as regulatory T cells (T_{reg}), and cell intrinsic mechanisms, such as inhibitory molecules that are upregulated on exhausted, tumor-infiltrating lymphocytes (TIL). In combination, these inhibitory mechanisms represent a formidable barrier to effective antitumor immunity (6–10).

Inhibitory receptors such as cytotoxic T-lymphocyte–associated protein 4 (CTLA-4, CD152), lymphocyte-activation gene 3 (LAG-3, CD223), and programmed cell death 1 (PD-1, CD279) function at multiple levels to ensure appropriate T-cell homeostasis, activation, and differentiation (7, 11–17). Furthermore, all 3 inhibitory molecules also contribute to cell extrinsic regulation by controlling T_{reg} homeostasis and function, mediating induced T_{reg} development, and mitigating dendritic cell differentiation and function (13–16, 18, 19). Data from genetically manipulated mice indicate that CTLA-4 represents a basic and indispensible "off switch," whereas PD-1 and LAG-3 play more subtle roles in immune regulation. Whereas $Ctla4^{-/-}$ mice develop a severe lymphoproliferative disease and are usually moribund by 3 to 4 weeks of age (20), $Pdcd1^{-/-}$

Authors' Affiliations: [1]Department of Immunology; [2]Veterinary Pathology Core; [3]Department of Biostatistics, St. Jude Children's Research Hospital, Memphis, Tennessee; [4]Departments of Oncology, Immunology and Urology; [5]Immunology and Hematopoiesis Division, Johns Hopkins Sidney Kimmel Comprehensive Cancer Center; [6]Departments of Oncology, Pathology and Urology; [7]Department of Pathology, Johns Hopkins University, Baltimore, Maryland; [8]Biologics Discovery California, Bristol-Myers-Squibb, Milpitas; and [9]Department of Medicine, Division of Immunology and Rheumatology, Stanford University School of Medicine, Stanford, California

Note: Supplementary data for this article are available at Cancer Research Online (http://cancerres.aacrjournals.org/).

Current address for Joseph F. Grosso: Clinical Biomarkers/Immuno-Oncology, Bristol-Myers-Squibb, Princeton, NJ.

S.-R. Woo, M.E. Turnis, and M.V. Goldberg contributed equally to this work.

C.G. Drake and D.A.A. Vignali share senior authorship.

Corresponding Authors: Dario A.A. Vignali, Department of Immunology, St. Jude Children's Research Hospital, Memphis, TN. Phone: 901-595-2576; Fax: 901-595-3107; E-mail: vignali.lab@stjude.org; and Charles G. Drake, Departments of Oncology, Immunology and Urology, Johns Hopkins Sidney Kimmel Comprehensive Cancer Center, Baltimore, MD. E-mail: cdrake@jhmi.edu

doi: 10.1158/0008-5472.CAN-11-1620

©2011 American Association for Cancer Research.

Downloaded from cancerres.aacrjournals.org on July 6, 2012
Copyright © 2012 American Association for Cancer Research

Published OnlineFirst December 20, 2011; DOI:10.1158/0008-5472.CAN-11-1620

(which encodes PD-1) mice live beyond 1 year while developing subtle and variable immune-based disease manifestations depending on genetic background; *Pdcd1*$^{-/-}$ BALB/c mice develop dilated cardiomyopathy 5 to 30 weeks of age, whereas *Pdcd1*$^{-/-}$ C57BL/6 mice develop a protracted lupus-like condition that takes over 6 months to develop (21, 22). Unmanipulated *Lag3*$^{-/-}$ C57BL/6 mice do not develop any disease manifestations within the first year of life (23).

Recent studies have revealed that LAG-3 and PD-1 are coexpressed on tolerized TILs suggesting that they may contribute to tumor-mediated immune suppression (5, 24). Preclinical models using antibody treatment to block LAG-3 for cancer treatment show enhanced activation of antigen-specific T cells at the tumor site and disruption of tumor growth (25). Abrogation of PD1 signaling in mice leads to enhanced CTL killing, cytokine production, and tumor-bearing animal survival over several different tumor models (26). On the basis of their roles in T-cell inhibition and antitumor immune regulation, individual antibody blockade of both CTLA-4 and PD-1 have been reported to show clinical utility (27, 28). Given this information, LAG-3 and PD-1 represent a potentially beneficial pairing for dual pathway blockade in cancer therapy. However, little is known about the extent of cooperative interaction between these regulatory pathways, information critical to the development of combinatorial immunotherapy based on simultaneous blockade of multiple receptors or ligands. In this study, we investigate whether there is synergy between LAG-3 and PD-1 by analysis of tumor growth and clearance in blocking antibody-treated mice and *Lag3*$^{-/-}$*Pdcd1*$^{-/-}$ mice.

Materials and Methods

Mouse strains and cell lines

C57BL/6 mice were purchased from The Jackson Laboratory. *Lag3*$^{-/-}$ mice were provided by Y.H. Chien (Stanford University) with permission from C. Benoist and D. Mathis (Joslin Diabetes Center; refs. 23, 29). *Pdcd1*$^{-/-}$ mice were provided by Lieping Chen (Johns Hopkins University) with permission from T. Honjo (Kyoto University; ref. 30). At St. Jude Children's Research Hospital, the *Lag3*$^{-/-}$, *Pdcd1*$^{-/-}$ and *Lag3*$^{-/-}$*Pdcd1*$^{-/-}$ mice were backcrossed onto a C57BL/6 background an additional 5, 9, and 5 generations respectively, and a genome-wide single-nucleotide polymorphism analysis indicated that 100% of the markers were C57BL/6 for *Lag3*$^{-/-}$ and *Pdcd1*$^{-/-}$ mice and 90% for the *Lag3*$^{-/-}$*Pdcd1*$^{-/-}$ mice. At Johns Hopkins, the *Lag3*$^{-/-}$*Pdcd1*$^{-/-}$ were backcrossed 5 generations onto a B10.D2 background and crossed with Clone 4 (CL4) TCR transgenic mice. Animal experiments were carried out in specific pathogen-free facilities accredited by the American Association for the Accreditation of Laboratory Animal Care (AAALAC) at St. Jude Children's Research Hospital and Johns Hopkins Kimmel Cancer Center and approved by the respective Animal Care and Use Committees. The mice at St. Jude Children's Research Hospital are also Helicobacter- and MNV free. B16 melanoma cells were obtained from MJ Turk (Dartmouth College, Hanover, NH). This line has been authenticated by the RADIL at the University of Missouri (September 18, 2008) and maintained in continuous culture for no more than 6 months posttesting. It was also tested by IMPACT I PCR Profile at the RADIL at the University of Missouri (October 10, 2008). MC38 cells were obtained from J.P. Allison (Memorial Sloan-Kettering Cancer Center, NY), authenticated by the RADIL (March 10, 2003), and tested by IMPACT I at the RADIL at the University of Missouri (March 18, 2010). Sa1N cells were originally obtained from J.P. Allison (Memorial Sloan-Kettering Cancer Center, NY). Although these cells have not been authenticated, they perform as described in the literature in syngeneic A/J mice (14) and tested by IMPACT I at the RADIL at the University of Missouri (January 29, 2011).

Flow cytometry, intracellular cytokine staining, and cytokine analysis

Single-cell suspensions were prepared from spleens, inguinal, brachial, and axillary lymph nodes, and tumors. Cells were stained with fluorescent-labeled antibodies (BioLegend, BD-Bioscience Pharmingen, or eBiosciences) and analyzed by either FACSCalibur or LSR II flow cytometer (BD). The following clones were used: CD4 (GK1.5), CD8α (53–6.7), CD11c (N418), CD25 (PC61), CD44 (IM7), CD45R/B220 (RA3–6B2), CD69 (H1.2F3), PD-1 (RMP1–30), TCR-β (H57–597), Thy1.1 (HIS51), IFN-γ (XMG1.2), TNF-α (MP6-XT22), IL-17 (TC11–18H10), Foxp3 (150D), and LAG-3 (4–10-C9; ref. 31). For intracellular cytokine staining, cells were activated with phorbol 12-myristate 13-acetate (PMA; 100 ng/mL) plus ionomycin (500 ng/mL) for 4 hours in the presence of GolgiPlug (32), processed with a Cytofix/Cytoperm kit (32), and stained as indicated. Measurement of IFN-γ, TNF-α, and MCP-1 in serum was determined by IFN-γ- or TNF-α–specific ELISA kits (eBioscience) and a MCP-1–specific bead based kit (Millipore).

Tumor growth experiments and TIL preparation

B16 melanoma and MC38 colon adenocarcinoma models were carried out as previously described with some modifications (33, 34). Briefly, on day 0 mice were injected with 1.25×10^5 to 5.0×10^5 B16 cells i.d. in the back or 2.0×10^6 to 5.0×10^6 MC38 cells subcutaneously (s.c) in the right flank. *Lag3*$^{-/-}$ *Pdcd1*$^{-/-}$ (and appropriate controls) were used at approximately 5 weeks of age. Tumor diameter was measured every 2 to 3 days with an electronic caliper and reported as volume using the formula $m_1^2 \times m_2 \times \pi/6$ (35). To isolate TILs, solid tumors were excised after 12 to 14 days, single-cell suspensions prepared by mechanical dissociation, followed by density gradient centrifugation on an 80%/40% Percoll (GE Healthcare) gradient. For CD4$^+$ and CD8$^+$ T-cell depletion experiments, anti-mouse CD4 (GK1.5) and anti-mouse CD8 (2.43) ascites were administered i.p. on days 1, 2, 5, 8, and 11 (pretitered for maximal deletion).

Dual antibody blocking experiments

Sa1N fibrosarcoma cells or MC38 cells (2×10^6) were implanted s.c. into A/J mice (Harlan) or C57Bl/6 mice (Charles River), respectively. Tumor volumes were measured with an electronic caliper ($l \times w \times h/2$) and randomized by size (10 mice per group). Mice with palpable tumors (Sa1N ~60 mm^3/2; MC38 ~40 mm^3/2) were injected i.p. at a dosage of 10 mg/kg for chimeric mouse anti-PD-1 (4H2, IgG1; ref. 36) and/or rat

Downloaded from cancerres.aacrjournals.org on July 6, 2012
Copyright © 2012 American Association for Cancer Research

Published OnlineFirst December 20, 2011; DOI:10.1158/0008-5472.CAN-11-1620

anti-mouse LAG-3 (C9B7W, IgG1; ref. 37). Control murine IgG1 (MOPC 21; BioXCell) was dosed at 20 mg/kg or added to individual anti–PD-1 or anti–LAG-3 antibody treatments at 10 mg/kg. Tumor growth inhibition (TGI) was calculated when all mice within a group were available for tumor measurement.

Adoptive transfer into Rag-1$^{-/-}$ mice

Splenocytes and lymph node cells from female mice (5–7 weeks old) were pooled, and 10^7 cells injected i.v. into age-matched female *Rag-1*$^{-/-}$ (5–6 weeks old) mice. CD4$^+$ or CD8$^+$ cells were depleted from splenocytes and lymph node cells with biotinylated anti-CD4 or anti-CD8 by macrophage separation using streptavidin-coupled beads (Milteny Biotec) to achieve purity above 95%.

Histopathology

Full necropsies were completed independently at St Jude Children's Research Hospital and Johns Hopkins. Tissues from knockout and control mice were fixed in 10% neutral buffered formalin, except eyes, which were fixed for 24 hours in Davidson's fixative, embedded in paraffin, sectioned at 4 μm and stained with hematoxylin and eosin for histopathologic examination. Collagen deposition was detected by a Masson's Trichrome stain. Macrophages and T cells were detected using rat anti-mouse MAC2 (CL8942AP; Accurate Chemical) and goat anti-human CD3 (sc-1127; Santa Cruz Biotechnology) antibodies, respectively. Heat-induced epitope retrieval was carried out by heating slides in ER2 (AR9640; Leica) for 30 minutes and the Refine system (DS9800; Leica Microsystems) used for detection. T_{reg} cells were detected with a rat anti-mouse FoxP3 antibody (14–5773-82; eBioscience) with heat-induced retrieval, pH 6.0, target retrieval buffer (S699; Dako) followed by a horseradish peroxidase–labeled streptavidin detection system (TS-125-HR; Thermo Shandon). In all immunohistochemical assays, 3,3′-diaminobenzidine was used as the chromogenic substrate with a light hematoxylin counterstain.

Autoantibody analysis

Mouse sera were analyzed by indirect ELISA, alongside a positive control (serum from a MRL/lpr mouse, a SLE disease model), using 96-well Nunc MaxiSorp plates (Nalgene Nunc). Multiple antigen blot assay (MABA) was conducted as described (38).

Clone 4 TCR transgenic T-cell experiments

CL4 adoptive transfer and *in vivo* CTL studies were carried out as previously described (25, 39).

Statistical analyses

Summary statistics are presented as mean ± SEM. Group means were compared with 2-sample *t* tests. Event-free survival (moribund) estimates were calculated with the Kaplan–Meier method; mouse groups were compared by log-rank test. The proportions of tumor-free mice were evaluated with the binomial distribution; synergy hypotheses were tested based on the maximum likelihood method. Trends in weight over time and tumor growth over time among different mice groups were analyzed using mixed models. All *P* values are 2-sided, and statistical significance was assessed at the 0.05 level. Analysis was conducted by SAS (version 9.2).

Results

Combinatorial anti–LAG-3/anti–PD-1 immunotherapy inhibits tumor growth

PD-1 monoclonal antibody treatment has shown clinical efficacy against multiple malignancies including melanoma, prostate, renal cell, and lung cancer (27). LAG-3 has been suggested to directly modulate the activity of PD-1$^+$ cells (5); furthermore, coexpression of LAG-3 and PD-1 has been shown in malignant mouse and human tissue (5, 24). Given these data, we hypothesized that LAG-3 and PD-1 act synergistically to control immune homeostasis and mediate tumor-induced tolerance. Consistent with previous reports, a significant percentage of CD4$^+$ and CD8$^+$ TILs from transplanted B16 melanoma, MC38 colorectal adenocarcinoma, and Sa1N fibrosarcoma expressed high levels of LAG-3 and PD-1 (32, 34), whereas similar upregulation was not observed on peripheral T-cell populations (Fig. 1). Next, we asked if antibody-mediated dual blockade of these pathways would reduce tumor growth by assessing the potential efficacy of combined anti–LAG-3 and anti–PD-1 blockade in mice with established tumors. Reduced growth of Sa1N fibrosarcoma and MC38 colorectal adenocarcinoma (32, 40–42) was observed in some but not all mice treated with the anti–LAG-3 or anti–PD-1 monotherapy (Fig. 2); only a few mice were tumor free after 50 days (0%–40%). For anti–LAG-3, this is the first demonstration of TGI with anti–LAG-3 as a monotherapy. In striking contrast, 70% and 80% of the Sa1N- and MC38-inoculated mice, respectively, were tumor free after 50 days following combinatorial anti–LAG-3/anti–PD-1 immunotherapy (Fig. 2). However, this regimen had no effect against established B16 tumors. Using the maximum likelihood method, there seemed to be a synergistic benefit of anti–LAG-3/anti–PD-1 combinatorial immunotherapy that is superior to either the additive effect of anti–LAG-3 and anti–PD-1 or monotherapy. Dual treatment with anti–LAG-3/anti–PD-1 did not result in immunopathologic manifestations such as lymphocytic infiltration in the Sa1N fibrosarcoma model as determined by detailed histologic analysis of multiple tissues. Despite efficient tumor clearance, no evidence of systemic or organ-specific autoimmunity was observed.

To investigate the mechanism underlying decreased tumor growth in antibody-treated mice, MC38 tumor-bearing mice were treated with the antibody combinations used above and draining lymph node (DLN) T cells, non-DLN (NDLN) T cells, and TILs analyzed by flow cytometry for phenotype and effector function. As expected, average tumor size of anti-PD1–treated or dual antibody–treated mice was significantly smaller than isotype control or anti-LAG3–treated mice (Supplementary Fig. S1). A significantly higher percentage of IFN-γ^+CD8$^+$ T cells were found in the tumor-associated DLNs of dual antibody–treated mice compared with the monotherapy groups, or cells analyzed from NDLNs (Fig. 3A). Likewise, a

Downloaded from cancerres.aacrjournals.org on July 6, 2012
Copyright © 2012 American Association for Cancer Research

Published OnlineFirst December 20, 2011; DOI:10.1158/0008-5472.CAN-11-1620

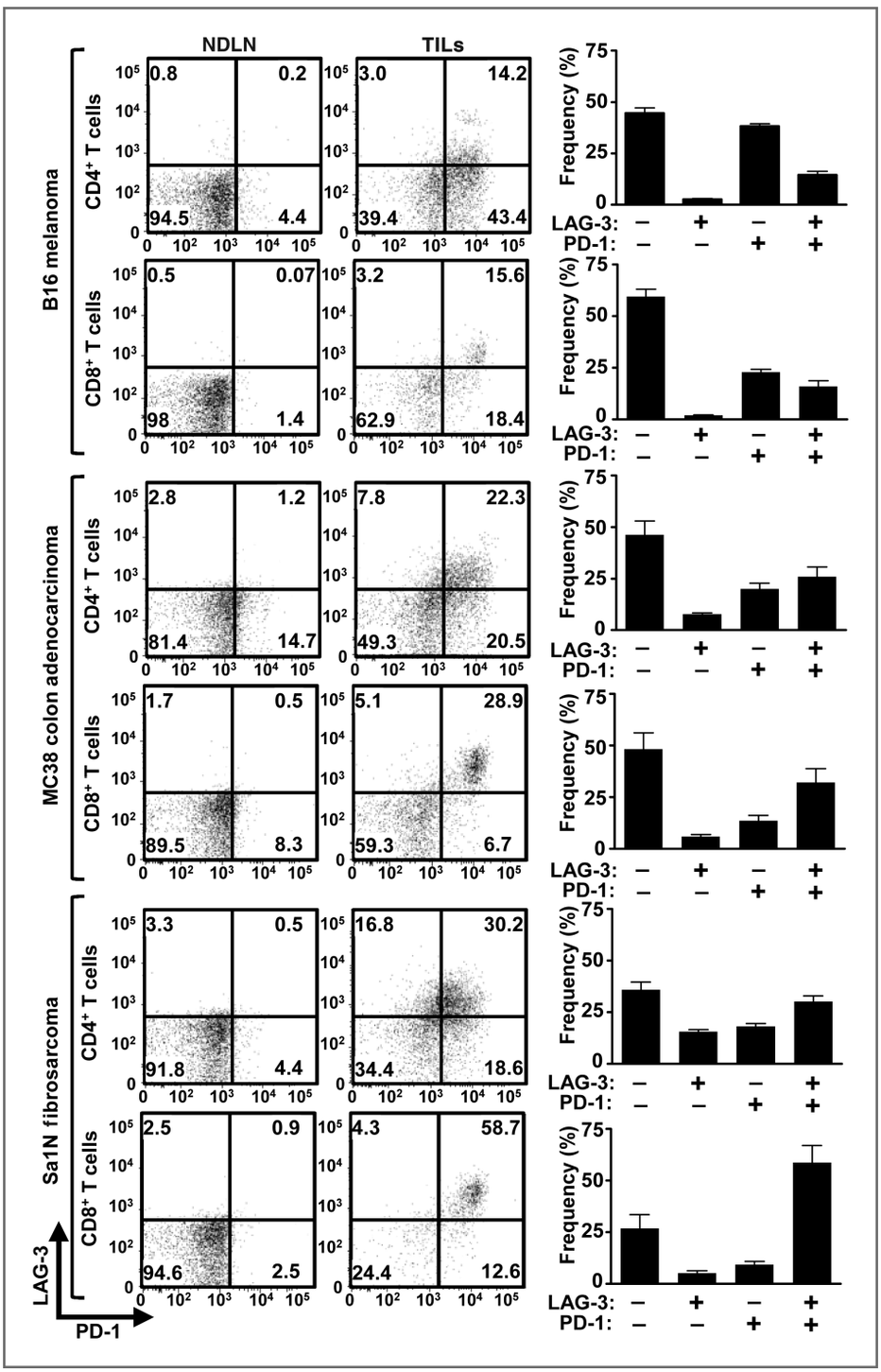

Figure 1. TILs express LAG-3 and PD-1. TILs were isolated from B16, MC38, and Sa1N tumors resected from wild-type mice 13 days postinoculation (average sizes: B16 = 350 mm^3, MC38 = 1000 mm^3, and Sa1N = 750 mm^3) and stained for flow cytometric analysis. Representative data (left; gated on live $CD4^+$ or $CD8^+$ lymphocytes as indicated) or pooled data (right; $n = 8–10$) of LAG-3/PD-1 expression on $CD4^+$ or $CD8^+$ TILs are shown.

higher percentage of IFN-γ^+CD4^+ and IFN-γ^+CD8^+ TILs, and to a lesser extent TNF-α^+ $CD4^+$ and $CD8^+$ TILs, were observed in anti–LAG-3/anti–PD-1–treated mice than in control groups (Fig. 3B). Taken together, these data suggest that anti–LAG-3/anti–PD-1 combinatorial immunotherapy may act synergistically to reduce tumor growth by increasing the proportion of effector T cells in the tumor and DLNs.

Lag3$^{-/-}$*Pdcd1*$^{-/-}$ mice develop lethal systemic autoimmunity

To further investigate the synergy between these 2 inhibitory molecules, we next assessed whether LAG-3 and PD-1 cooperate to control immune homeostasis and mediate tumor-induced tolerance with a genetic approach. *Lag3*$^{-/-}$*Pdcd1*$^{-/-}$ C57BL/6 or B10.D2 mice were generated at 2 independent

Downloaded from cancerres.aacrjournals.org on July 6, 2012
Copyright © 2012 American Association for Cancer Research

Published OnlineFirst December 20, 2011; DOI:10.1158/0008-5472.CAN-11-1620

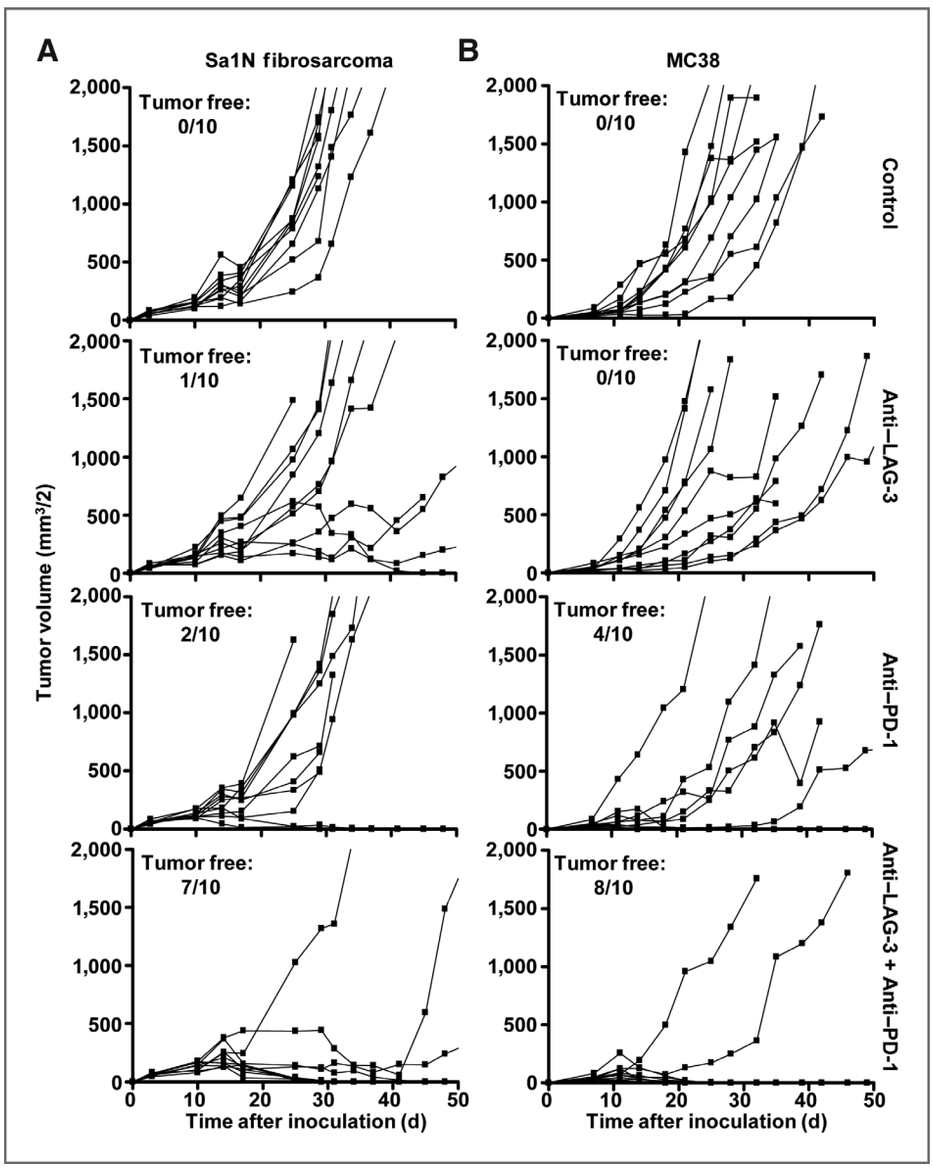

Figure 2. Combinatorial anti–LAG-3/anti–PD-1 treatment inhibits tumor growth. Mice [A/J (A); C57BL/6 (B)] were randomized on (A) on day 6 when Sa1N fibrosarcoma tumor volumes were approximately 60 $mm^3/2$, or (B) on day 7 when MC38 colon adenocarcinoma tumor volumes were approximately 40 $mm^3/2$, and treated with isotype control, anti-PD-1, anti-LAG-3, or anti-PD-1/LAG-3 combination on days 8, 11, and 14 and tumor volume determined. TGI on day 18: (A) anti–LAG-3: 18.9%; anti–PD-1: 26.2%; anti–PD-1/LAG-3: 77.3%. B, anti–LAG-3: 1%; anti–PD-1: 55%; anti–PD-1/LAG-3: 79%. Data represent 3 (Sa1N) or 4 (MC38) repeated experiments with 10 mice per group. Data were analyzed by the Maximum Likelihood method to determine synergy *P* values: (A) 0.0622 (for experiment shown; 0.0002 with all 3 experiments combined) and (B) 0.0455 (for experiment shown; 0.0366 with all 4 experiments combined) for the anti–PD-1/LAG-3 combinatorial treatment compared with anti–PD-1 and anti–LAG-3 treatments alone.

locations (see Materials and Methods), and disease manifestation and immune pathology analyzed over time. *Lag3*$^{-/-}$*Pdcd1*$^{-/-}$ mice developed an early onset (~4 weeks of age), lethal autoimmune condition that resulted in approximately 80% of the mice moribund by approximately 10 weeks (Fig. 4A and Supplementary Fig. S2). The major histopathologic manifestations included diffuse fibrosing lymphohistiocytic endocarditis, myocarditis, and pancreatitis (Fig. 4B, Supplementary Table S1 and Fig. S3). Extensive infiltration by CD3$^+$ T cells, Foxp3$^+$ T_{reg} cells, and Mac2$^+$-F4/80$^+$ macrophages was observed, in conjunction with substantial collagen deposition but limited B-cell and neutrophil infiltration; however, negligible autoantibody reactivity was seen in serum from *Lag3*$^{-/-}$*Pdcd1*$^{-/-}$ mice but not single knockout or wild-type mice (Supplementary Fig. S4). *Lag3*$^{-/-}$ and *Pdcd1*$^{-/-}$ single KO mice lacked any disease manifestations or histopathology over this period of observation. These results show that the PD-1 and LAG-3 pathways synergistically regulate self-reactivity.

Consistent with the histopathology observed, substantially increased numbers of CD4$^+$ and CD8$^+$ T cells were observed in the regional LNs, but not the spleens, of *Lag3*$^{-/-}$*Pdcd1*$^{-/-}$ mice (Fig. 4C, Supplementary Fig. S5). These cells possessed a predominantly activated/memory phenotype as indicated by CD69/CD44 staining. Nevertheless, there seemed to be minimal difference in the extent of division *in vivo* based on *ex vivo* Ki67 staining, even though *Lag3*$^{-/-}$*Pdcd1*$^{-/-}$ T cells proliferate more *in vitro* following anti-CD3 stimulation (data not shown). The number of CD4$^+$Foxp3$^+$ T_{reg} cells, B cells, and CD11c$^+$ dendritic cells were also increased in *Lag3*$^{-/-}$*Pdcd1*$^{-/-}$ mice (Fig. 4C, Supplementary Fig. S5). Given that *Lag3*$^{-/-}$ T_{reg} cells exhibit reduced suppressive activity (13, 14) and PD-L1 (PD-1 ligand)

Downloaded from cancerres.aacrjournals.org on July 6, 2012
Copyright © 2012 American Association for Cancer Research

Published OnlineFirst December 20, 2011; DOI:10.1158/0008-5472.CAN-11-1620

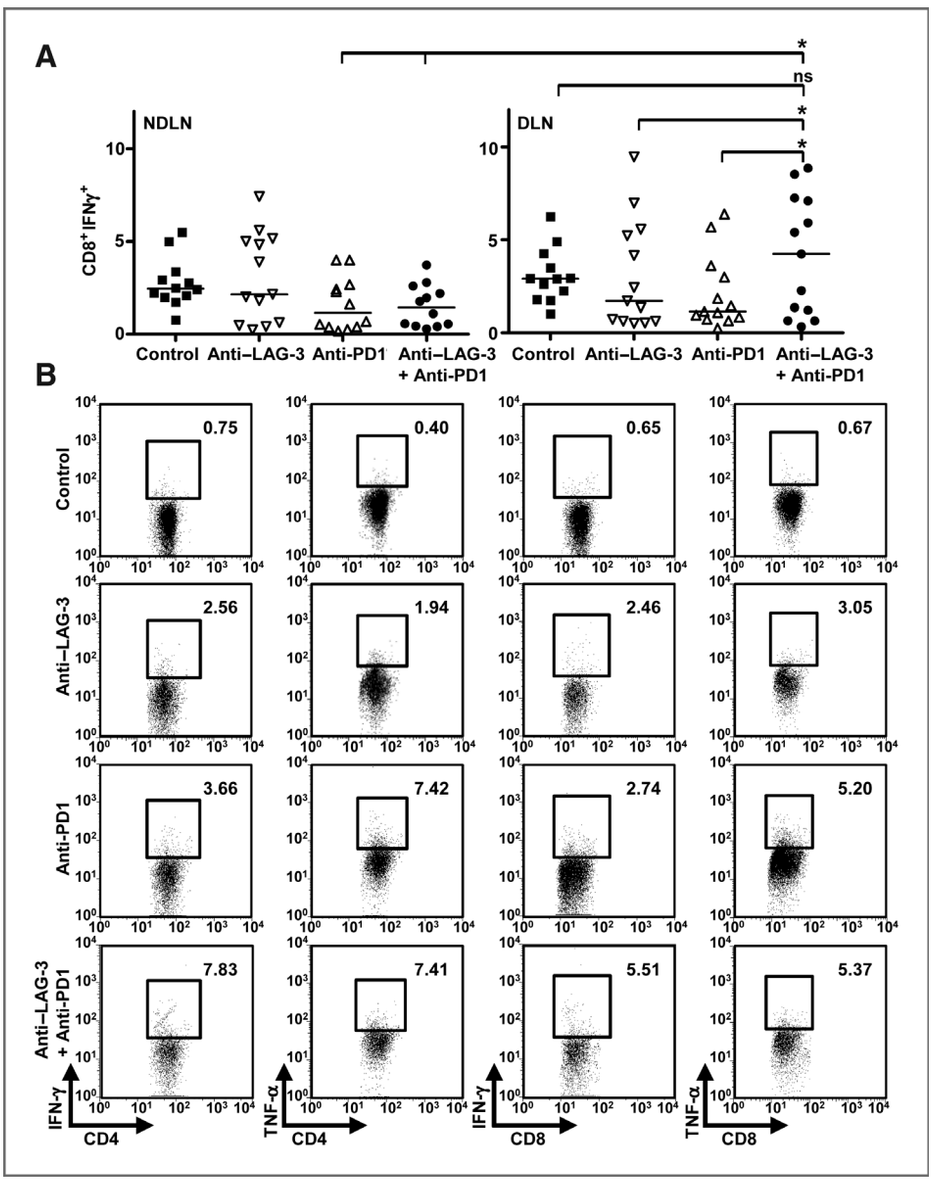

Figure 3. Combinatorial anti–LAG-3/anti–PD-1 treatment results in enhanced adaptive immune responses. Mice were inoculated on day 0 with 2×10^6 MC38 cells s.c. in the right flank, euthanized at day 15, and tissues analyzed by flow cytometry. A, tumor draining inguinal (DLN) and nondraining brachial and axillary lymph nodes (NDLN) were isolated and activated with PMA + ionomycin for 4 hours in the presence of brefeldin A, then analyzed by intracellular staining and flow cytometry (gated on lymphocytes). Nonparametric 1-way ANOVA with Kruskal–Wallis test ($P = 0.0074$) was used for part A. B, TILs were analyzed by intracellular staining and flow cytometry; plots represent 5 to 8 animals per group. Numbers are percentage cytokine-positive infiltrating lymphocytes.

contributes to iT_{reg} development (15), it is possible that the combined loss of LAG-3 and PD-1 alters T_{reg} cell homeostasis.

To further probe the cellular defects in *Lag3*$^{-/-}$*Pdcd1*$^{-/-}$ mice, we adoptively transferred splenocytes into lymphopenic *Rag-1*$^{-/-}$ mice. In contrast to healthy wild-type and single knockout controls, *Lag3*$^{-/-}$*Pdcd1*$^{-/-}$ splenocyte recipients started to lose body weight approximately 6 days posttransfer with 100% morbidity by day 20 (Supplementary Fig. S6A and S6B). Adoptive transfer experiments T-cell–depleted *Lag3*$^{-/-}$*Pdcd1*$^{-/-}$ splenocytes clearly showed that both CD4$^+$ or CD8$^+$ T-cell populations contributed to the disease observed, with a dominant role for the former (Supplementary Fig. S6C and S6D). Consistent with these survival and weight loss data, histologic analysis of CD4$^+$ T-cell–depleted *Lag3*$^{-/-}$*Pdcd1*$^{-/-}$ splenocyte recipients revealed relatively normal bone marrow cellularity and density, whereas *Lag3*$^{-/-}$*Pdcd1*$^{-/-}$ splenocyte recipients exhibited a near total absence of hematopoietic cell precursors in bone marrow and severe lymphoid depletion in the spleen, LNs, and Peyer's patches (Supplementary Table S2, Fig. S6E and S7). These data indicate that CD4$^+$ T cells are primarily responsible for the pathology observed. Cytokine analysis revealed high levels of IFN-γ, TNF-α, and MCP-1 in the serum of *Lag3*$^{-/-}$*Pdcd1*$^{-/-}$ recipients but not single knockout or wild-type control recipients (Supplementary Fig. S6F–S6H). Taken together, these data suggest that *Lag3*$^{-/-}$*Pdcd1*$^{-/-}$ splenocyte recipients, in contrast with their single knockout and wild-type controls, develop an autoimmune GvHD-like syndrome with evidence of aplastic anemia and bone marrow failure as a cause of death.

The data thus far suggested that while a reasonable level of tolerance is maintained in single knockout *Lag3*$^{-/-}$ or *Pdcd1*$^{-/-}$ mice, dual loss of LAG-3 and PD-1 expression results

Downloaded from cancerres.aacrjournals.org on July 6, 2012
Copyright © 2012 American Association for Cancer Research

Published OnlineFirst December 20, 2011; DOI:10.1158/0008-5472.CAN-11-1620

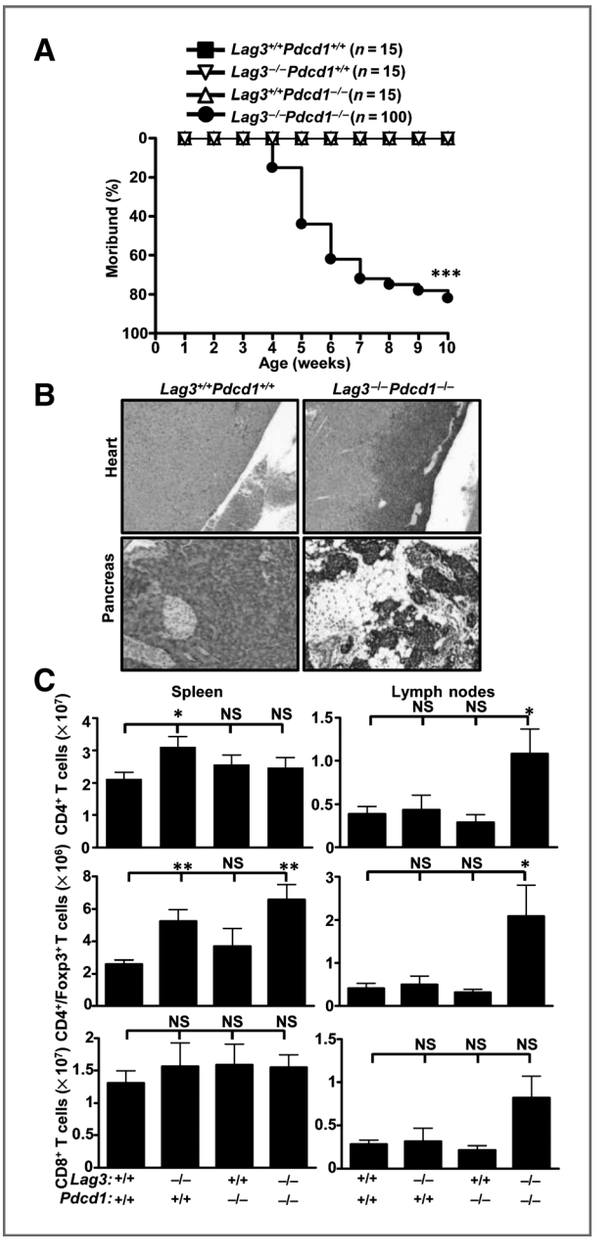

Figure 4. *Lag3*$^{-/-}$*Pdcd1*$^{-/-}$ mice develop lethal systemic autoimmunity. A, disease incidence for *Lag3*$^{-/-}$*Pdcd1*$^{-/-}$ mice, plus single knockout and WT littermate controls. Moribund curves were analyzed for statistical significance by log-rank test; ***, $P < 0.001$. B, representative histopathology of the heart and pancreas of WT and *Lag3*$^{-/-}$*Pdcd1*$^{-/-}$ mice. C, number of various T-cell populations in the spleen and LNs (inguinal and brachial) is shown. Data represent 3 to 4 independent experiments with 4 to 7 mice total per group (5- to 7 weeks old). Error bars represent SEM; *, $P < 0.05$; **, $P < 0.01$ (unpaired *t* test).

in a loss of peripheral self-tolerance of CD4$^+$ and CD8$^+$ T cells. To test this in an antigen-specific system, we asked whether hemagglutinin-specific tolerance induced in transgenic mice expressing hemagglutinin as a self-antigen in multiple epithelial tissues (C3-HA^{lo} mice; refs. 13, 43), could also be broken if adoptively transferred hemagglutinin-specific T cells [from Clone 4 (CL4) TCR transgenics] lacked both inhibitory molecules. Compared with wild-type CL4 T cells, significant expansion of *Lag3*$^{-/-}$*Pdcd1*$^{-/-}$ clonotypic CD8$^+$ T cells was observed 5 days posttransfer (Supplementary Fig. S6I). Although this was not substantially greater than that seen with *Pdcd1*$^{-/-}$ T cells, the *Lag3*$^{-/-}$*Pdcd1*$^{-/-}$ T cells exhibited a significantly enhanced effector phenotype, as determined by intracellular expression of IFN-γ and IL-17, compared with their single knockout and wild-type controls (Supplementary Fig. S6J and S6K). Similarly, when tolerance was broken in C3-HA^{lo} transgenic mice (39), adoptive transfer of antigen-specific *Lag3*$^{-/-}$*Pdcd1*$^{-/-}$ CD8$^+$ T cells expanded significantly more than their single knockout and wild-type controls, although enhanced *in vivo* CTL activity was comparable in the *Pdcd1*$^{-/-}$ and *Lag3*$^{-/-}$*Pdcd1*$^{-/-}$ CD8$^+$ T cell recipients (Supplementary Fig. S8). Collectively, these data suggest that the loss of LAG-3 and PD-1 also results in loss of tolerance to a model self-antigen.

Reduced tumor growth and enhanced survival in *Lag3*$^{-/-}$*Pdcd1*$^{-/-}$ mice

To continue our analysis of Lag-3/PD-1 synergy in the regulation of antitumor immunity, we assessed tumor growth in *Lag3*$^{-/-}$*Pdcd1*$^{-/-}$ mice and controls over time. Of the 3 transplantable tumor models examined in this study, B16 is regarded as the least immunogenic and thus the hardest to eliminate by immunologic intervention (32, 34). A low dose of B16 cells (1.25×10^5) progressively grew in wild-type and *Lag3*$^{-/-}$ mice inoculated intradermally at day 0, whereas limited growth was observed in *Pdcd1*$^{-/-}$ and *Lag3*$^{-/-}$*Pdcd1*$^{-/-}$ mice (Supplementary Fig. S9A). Although previous studies suggested that PD-1 deletion did not affect subcutaneously injected tumor growth (44), our experiments revealed reduced tumor growth in *Pdcd1*$^{-/-}$ mice compared with wild-type mice. Paradoxically, *Lag3*$^{-/-}$ mice developed slightly larger tumors. Whether this is due to reported defects in natural killer cell cytolysis (23), or an unexpected role of pDCs, which highly express LAG-3 (45), remains to be determined. Statistical analysis with the maximum likelihood method for synergy found that the lack of tumor growth in the *Lag3*$^{-/-}$*Pdcd1*$^{-/-}$ mice was greater than the additive effects of tumor growth in *Lag3*$^{-/-}$ mice and *Pdcd1*$^{-/-}$ mice at day 11 ($P < 0.05$) and day 13 ($P < 0.0005$) suggesting that LAG-3 and PD-1 synergize to mediate tumor-induced tolerance. Depletion of CD4$^+$ and CD8$^+$ T cells restored normal B16 tumor growth in compound-deficient mice, indicating the necessity of adaptive immunity to the antitumor response (Supplementary Fig. S9B).

As the difference in resistance to B16 growth between *Pdcd1*$^{-/-}$ and *Lag3*$^{-/-}$*Pdcd1*$^{-/-}$ mice seemed small, we evaluated tumor B16 and MC38 growth at different doses. At the higher B16 dose (5×10^5 cells per mouse), wild-type and *Lag3*$^{-/-}$ mice show uncontrolled tumor growth and lethality with an average survival time of less than 20 days (Fig. 5A and Supplementary Fig. S10). *Lag3*$^{-/-}$*Pdcd1*$^{-/-}$ mice (80%) eliminated tumors compared with only 40% of *Pdcd1*$^{-/-}$ mice; however, B16 survivors did not display autoimmune vitiligo as is often seen with this model (46). We also investigated growth of subcutaneously implanted MC38 adenocarcinoma cells at 2 different doses. Whereas MC38 growth and survival were

Downloaded from cancerres.aacrjournals.org on July 6, 2012
Copyright © 2012 American Association for Cancer Research

Published OnlineFirst December 20, 2011; DOI:10.1158/0008-5472.CAN-11-1620

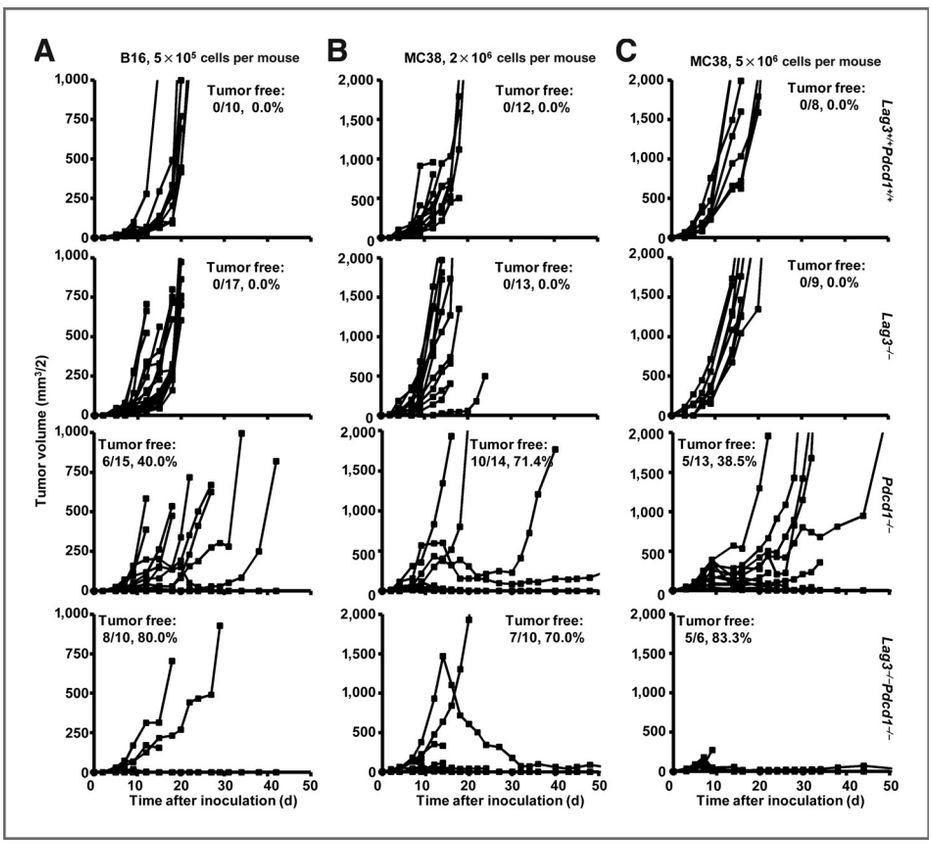

Figure 5. Reduced tumor growth in tumor-bearing *Lag3*$^{-/-}$*Pdcd1*$^{-/-}$ mice. Wild type, *Lag3*$^{-/-}$, *Pdcd1*$^{-/-}$, and *Lag3*$^{-/-}$*Pdcd1*$^{-/-}$ mice were inoculated on day 0 with 5×10^5 B16 cells i.d. (A), 2×10^6 MC38 cells s.c. (B), or 5×10^6 MC38 cells s.c. (C). Tumors were measured with an electronic caliper and reported as volume (see Materials and Methods). Data are combined from 2 to 3 repeated experiments, 3 to 5 animals per animals per group. Data were analyzed by the Maximum Likelihood method to determine synergy p values: 0.0253 (A), 0.94 (B), and 0.0273 (C) for the *Lag3*$^{-/-}$*Pdcd1*$^{-/-}$ mice compared with the additive effect of the 2 single knockouts. Animals were euthanized when tumors became large, ulcerated, and/or necrotic.

comparable in *Lag3*$^{-/-}$*Pdcd1*$^{-/-}$ and *Pdcd1*$^{-/-}$ mice when a low dose (2×10^5 cells per mouse) was used (70% vs. 71%, respectively; Fig. 5B and Supplementary Fig. S10), *Lag3*$^{-/-}$*Pdcd1*$^{-/-}$ mice were clearly more effective at preventing high-dose (5×10^5 cells per mouse) MC38 tumor growth and ensuring survival (83% vs. 38%, respectively; Fig. 5C and Supplementary Fig. S10). Phenotypic analysis revealed enhanced IFN-γ expression by *Lag3*$^{-/-}$*Pdcd1*$^{-/-}$ CD4$^+$ and CD8$^+$ T cells in tumor DLNs compared with wild-type and *Lag3*$^{-/-}$ mice, and NDLNs from all groups (Fig. 6). These data suggest that combined loss of LAG-3 and PD-1 limits tumor-mediated tolerization and enhances tumor-specific immunity and resistance to tumor growth.

To further investigate the killing efficacy of *Lag3*$^{-/-}$*Pdcd1*$^{-/-}$ T cells *in vivo* in the presence of an established tumor, clonotypic CL4 CD8$^+$ T cells were transferred into ProTRAMP male mice, which develop prostate cancer driven by the probasin promoter and express hemagglutinin. After vaccination with hemagglutinin-expressing Vaccinia virus, *Lag3*$^{-/-}$*Pdcd1*$^{-/-}$ recipients showed significantly increased killing ability in comparison with the wild type, and slightly increased killing efficiency in comparison with *Pdcd1*$^{-/-}$ single knockouts (Supplementary Fig. S11). These data support the conclusion that *Lag3*$^{-/-}$*Pdcd1*$^{-/-}$ CD8$^+$ T cells are less susceptible to tumor-induced tolerance than wild-type cells. Taken together, these data clearly show that *Lag3*$^{-/-}$*Pdcd1*$^{-/-}$ mice are more capable of resisting high-dose tumor growth than *Pdcd1*$^{-/-}$ and wild-type mice.

Discussion

The data presented here illustrate clear synergy between the inhibitory receptors LAG-3 and PD-1 in controlling immune homeostasis, preventing autoimmunity, and enforcing tumor-induced tolerance. First, we show coexpression of LAG-3 and PD-1 on tumor-infiltrating lymphocytes. Second, we show that dual blockade of these receptors leads to decreased tumor growth and enhanced antitumor immunity. Importantly, dual antibody–treated mice show more robust immune responses than either single-treated group. Third, analysis of mutant mice revealed a cooperative requirement for LAG-3 and PD-1 in maintaining immune homeostasis. Consistent with our observations following antibody-mediated blockade of LAG-3 and PD-1, *Lag3*$^{-/-}$*Pdcd1*$^{-/-}$ mice prevented growth of high-dose B16 and MC38 tumors and ensured survival while single knockout controls and wild-type mice succumbed to disease. Taken together, these data reveal an unappreciated synergistic cooperation between LAG-3 and PD-1 in limiting tumor growth.

Although anti–LAG-3/anti–PD-1 combinatorial immunotherapy effectively cleared established Sa1N and MC38 tumors, this therapy was not effective against established B16 tumors. In contrast, B16 tumors were more difficult to establish in *Lag3*$^{-/-}$*Pdcd1*$^{-/-}$ mice. B16 is a more difficult tumor to eradicate than MC38 and Sa1N and thus there could be several possible explanations for this apparent discrepancy. First, expression of LAG-3/PD-1 on TILs from B16 is lower than for

Downloaded from cancerres.aacrjournals.org on July 6, 2012
Copyright © 2012 American Association for Cancer Research

Published OnlineFirst December 20, 2011; DOI:10.1158/0008-5472.CAN-11-1620

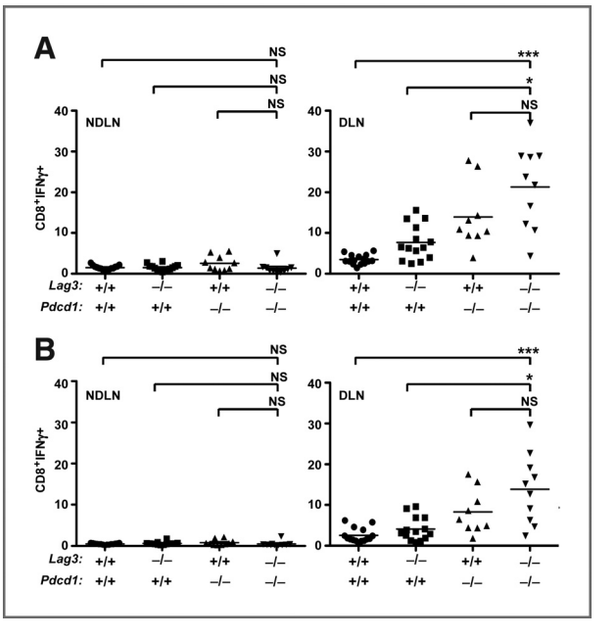

Figure 6. Tumor-draining (DLN; right) and nondraining (NDLN; left) LN T cells were isolated on day 14 post-B16 inoculation and were activated with PMA + ionomycin for 4 hours in the presence of brefeldin A. After intracellular cytokine staining, $CD8^+IFN\text{-}\gamma^+$ (A) and $CD4^+IFN\text{-}\gamma^+$ (B) cells were analyzed by flow cytometry. Data are representative of 10 to 15 animals per group. Nonparametric 1-way ANOVA with Kruskal–Wallis test ($P < 0.0001$) was used; *, $P < 0.05$; **, $P < 0.01$; and ***, $P < 0.001$ vs. *Lag3*$^{-/-}$*Pdcd1*$^{-/-}$.

MC38 and Sa1N, and this may be below a required threshold for efficacy upon antibody blockade in tumor-bearing mice. Second, as the knockout mice would lack LAG-3/PD-1 at the initiation of tumor inoculation, the immune system would not have this impediment at the commencement of an antitumor response. In contrast, the initial stages of LAG-3/PD-1 upregulation may already have occurred in tumor-bearing mice at the time of antibody treatment thereby establishing sufficient tolerance to prevent effective antitumor immunity. Third, there may be additional regulatory mechanisms that contribute a greater role with B16 that may be sufficient to prevent antitumor immunity when LAG-3/PD-1 blockade is initiated in mice that already have tumors. Lastly, we cannot rule out the possibility that the genetic deletion of LAG-3/PD-1 results in T_{regs} that have a cell intrinsic defect in their regulatory capacity which impacts early tumor establishment. Of course, a combination of these issues could also contribute to the difference in B16 clearance seen in LAG-3/PD-1 deficiency versus late stage antibody-mediated blockade. It is possible that alternate dosing regimens and therapeutic combinations could result in effective clearance of established B16 with anti–LAG-3/anti–PD-1 combinatorial immunotherapy.

It is noteworthy that the percentage of $IFN\text{-}\gamma^+$ TILs is higher in *Lag3*$^{-/-}$*Pdcd1*$^{-/-}$ mice versus anti–LAG-3/anti–PD-1–treated mice (Fig. 6 vs. Fig. 3). These differences could be reflective of the differences in B16 elimination in LAG-3/PD-1–deficient versus mAb-treated mice. Alternatively, as discussed above, these observations could be due to the different tumors analyzed or temporal differences between these experiments, as IFN-γ expression was determined 1 week after mAb treatment compared with 2 weeks after tumor inoculation into *Lag3*$^{-/-}$*Pdcd1*$^{-/-}$ mice. Finally, we cannot rule out the possibility that there is a phenotypic difference in the immune cells in the *Lag3*$^{-/-}$*Pdcd1*$^{-/-}$ mice. However, there does not seem to be an active systemic defect at the time of the experiment as high IFN-γ expression is not observed in the NDLN.

Although *Lag3*$^{-/-}$*Pdcd1*$^{-/-}$ mice develop a lethal autoimmune condition, the disease is slower (~10 weeks vs. 3–4 weeks) and less penetrant (80% vs. 100%) than the phenotype observed in *Ctla4*$^{-/-}$ mice (20). Recently, analogous observations were reported by Honjo and colleagues in which BALB/c mice harboring a loss-of-function mutation in *Lag3* combined with genetic deletion of *Pdcd1* develop lethal myocarditis (47). Heart-infiltrating T cells from these compound-deficient mice were shown to produce high amounts of IFNγ compared with distal lymphoid organs such as the spleen. Our results are consistent with their data, as we also observed enhanced production of proinflammatory cytokines by T cells infiltrating sites of inflammation, such as the heart and pancreas in *Lag3*$^{-/-}$*Pdcd1*$^{-/-}$ mice and in tumors and DLNs in knockout and antibody-treated mice. Furthermore, the Honjo group also observed accelerated autoimmune diabetes in NOD mice expressing a loss-of-function *LAG-3* mutant, consistent with our recent observations in *Lag3*$^{-/-}$ NOD mice (48). However, the mice used by Honjo and colleagues that lacked functional LAG-3/PD-1 expression were on a BALB/c background, whereas our data were derived from mice on a C57BL/6 or B10.D2 background. Strain-specific differences between these mice have been well documented (49, 50) and may have contributed to subtle differences in phenotypic and mechanistic observations reported. For instance, loss of LAG-3/PD-1 on a B10.D2 background can lead to an increase in $IL\text{-}17^+$ cells which was not seen in mice on a Balb/c background.

Although CTLA-4, PD-1, and LAG-3 are all negative regulators expressed during T-cell activation, high level, dual LAG-3/PD-1 expression is largely restricted to infiltrating TILs. Thus, LAG-3/PD-1 combinatorial immunotherapy may promote tumor-specific responses relative to nonspecific or self-antigen–specific immune responses and thus may be less toxic than CTLA-4 blockade. Given the recent phase 3 results with anti–CTLA-4 treatment of patients with metastatic melanoma, showing a clear survival benefit (albeit with notable immune toxicity; ref. 28), our results suggest that combined blockade of PD-1 and LAG-3 is a highly promising combinatorial strategy for the immune-based therapy of cancer.

Disclosure of Potential Conflict of Interest

The authors declare competing financial interests. D.M. Pardoll, D.A.A. Vignali, C.G. Drake, and C.J. Workman have submitted patents that are pending and are entitled to a share in net income generated from licensing of these patent rights for commercial development. A.J. Korman, M. Selby, and J.F. Grosso are employees of Bristol-Myers Squibb. C.G. Drake has an ownership interest in Amplimmune and has served as a consultant to Dendreon, Bristol-Myers Squibb, and Pfizer.

Downloaded from cancerres.aacrjournals.org on July 6, 2012
Copyright © 2012 American Association for Cancer Research

Published OnlineFirst December 20, 2011; DOI:10.1158/0008-5472.CAN-11-1620

Acknowledgments

The authors thank Many Jo Turk and Jim Allison for cell lines. At St. Jude, the authors thank Karen Forbes, Amy Krause, and Ashley Castellaw for maintenance and breeding of mouse colonies, Cliff Guy for help with cytokine analysis, Paul Thomas for anti-CD4 and anti-CD8 depleting Abs, Richard Cross, Greig Lennon and Stephanie Morgan for FACS, Song Wu and Hui Zhang for help with statistical analysis, the staff of the Shared Animal Resource Center at St Jude for the animal husbandry, the Veterinary Pathology Core Laboratory at St. Jude for histology and immunohistochemistry support, and the Hartwell Center for Biotechnology and Bioinformatics at St Jude for real-time PCR primer/probe synthesis and MOG synthesis and purification. At Johns Hopkins, the authors thank Dih-Dih Huang for the maintenance and breeding of the mouse colonies, and technical support. At Bristol-Myers-Squibb, the authors thank David Klitzing and the staff of the Milpitas animal facility for carrying out the tumor experiments and Rangan Vanganipuram, Brian Lee, and Shilpa Mankikar for provision of antibodies.

Grant Support

This work was supported by the NIH (R01 AI39480 to D.A.A. Vignali and R01 CA127153 and P50 CA58236–15 to C.G. Drake), a Hartwell Postdoctoral Fellowship (to M.L. Bettini), NCI Comprehensive Cancer Center Support CORE grant (CA21765, to D.A.A. Vignali), the American Lebanese Syrian Associated Charities (ALSAC, to D.A.A. Vignali), the Patrick C. Walsh Fund (to C.G. Drake), the Koch Fund (to C.G. Drake), NHLBI contract - HHSN-268201999934C and CIHR - 20R92141 to P.J. Utz, and NIAID F32 AI080086 to C.L. Liu. C.G. Drake is a Damon Runyon-Lilly Clinical Investigator.

The costs of publication of this article were defrayed in part by the payment of page charges. This article must therefore be hereby marked *advertisement* in accordance with 18 U.S.C. Section 1734 solely to indicate this fact.

Received May 11, 2011; revised December 7, 2011; accepted December 10, 2011; published OnlineFirst December 20, 2011.

References

1. Vesely MD, Kershaw MH, Schreiber RD, Smyth MJ. Natural innate and adaptive immunity to cancer. Annu Rev Immunol 2011;29:235–71.
2. Dunn GP, Bruce AT, Ikeda H, Old LJ, Schreiber RD. Cancer immunoediting: from immunosurveillance to tumor escape. Nat Immunol 2002;3:991–8.
3. Leen AM, Rooney CM, Foster AE. Improving T cell therapy for cancer. Annu Rev Immunol 2007;25:243–65.
4. Blackburn SD, Shin H, Haining WN, Zou T, Workman CJ, Polley A, et al. Coregulation of CD8$^+$ T cell exhaustion by multiple inhibitory receptors during chronic viral infection. Nat Immunol 2009;10:29–37.
5. Matsuzaki J, Gnjatic S, Mhawech-Fauceglia P, Beck A, Miller A, Tsuji T, et al. Tumor-infiltrating NY-ESO-1-specific CD8$^+$ T cells are negatively regulated by LAG-3 and PD-1 in human ovarian cancer. Proc Natl Acad Sci U S A 2010;107:7875–80.
6. Driessens G, Kline J, Gajewski TF. Costimulatory and coinhibitory receptors in anti-tumor immunity. Immunol Rev 2009;229:126–44.
7. Fife BT, Pauken KE, Eagar TN, Obu T, Wu J, Tang Q, et al. Interactions between PD-1 and PD-L1 promote tolerance by blocking the TCR-induced stop signal. Nat Immunol 2009;10:1185–92.
8. Francisco LM, Sage PT, Sharpe AH. The PD-1 pathway in tolerance and autoimmunity. Immunol Rev 2010;236:219–42.
9. Goldberg MV, Drake CG. LAG-3 in cancer immunotherapy. Curr Top Microbiol Immunol 2010;344:269–78.
10. Vignali DA, Collison LW, Workman CJ. How regulatory T cells work. Nat Rev Immunol 2008;8:523–32.
11. Workman CJ, Dugger KJ, Vignali DA. Cutting edge: molecular analysis of the negative regulatory function of lymphocyte activation gene-3. J Immunol 2002;169:5392–5.
12. Okazaki T, Honjo T. The PD-1-PD-L pathway in immunological tolerance. Trends Immunol 2006;27:195–201.
13. Huang CT, Workman CJ, Flies D, Pan X, Marson AL, Zhou G, et al. Role of LAG-3 in regulatory T cells. Immunity 2004;21:503–13.
14. Workman CJ, Vignali DA. Negative regulation of T cell homeostasis by lymphocyte activation gene-3 (CD223). J Immunol 2005;174:688–95.
15. Francisco LM, Salinas VH, Brown KE, Vanguri VK, Freeman GJ, Kuchroo VK, et al. PD-L1 regulates the development, maintenance, and function of induced regulatory T cells. J Exp Med 2009;206:3015–29.
16. Ise W, Kohyama M, Nutsch KM, Lee HM, Suri A, Unanue ER, et al. CTLA-4 suppresses the pathogenicity of self antigen-specific T cells by cell-intrinsic and cell-extrinsic mechanisms. Nat Immunol 2010;11:129–35.
17. Chambers CA, Sullivan TJ, Allison JP. Lymphoproliferation in CTLA-4-deficient mice is mediated by costimulation-dependent activation of CD4$^+$ T cells. Immunity 1997;7:885–95.
18. Wing K, Onishi Y, Prieto-Martin P, Yamaguchi T, Miyara M, Fehervari Z, et al. CTLA-4 control over Foxp3$^+$ regulatory T cell function. Science 2008;322:271–5.
19. Liang B, Workman C, Lee J, Chew C, Dale BM, Colonna L, et al. Regulatory T cells inhibit dendritic cells by lymphocyte activation gene-3 engagement of MHC class II. J Immunol 2008;180:5916–26.
20. Waterhouse P, Penninger JM, Timms E, Wakeham A, Shahinian A, Lee KP, et al. Lymphoproliferative disorders with early lethality in mice deficient in Ctla-4. Science 1995;270:985–8.
21. Nishimura H, Nose M, Hiai H, Minato N, Honjo T. Development of lupus-like autoimmune diseases by disruption of the PD-1 gene encoding an ITIM motif-carrying immunoreceptor. Immunity 1999;11:141–51.
22. Nishimura H, Okazaki T, Tanaka Y, Nakatani K, Hara M, Matsumori A, et al. Autoimmune dilated cardiomyopathy in PD-1 receptor-deficient mice. Science 2001;291:319–22.
23. Miyazaki T, Dierich A, Benoist C, Mathis D. Independent modes of natural killing distinguished in mice lacking Lag3. Science 1996;272:405–8.
24. Grosso JF, Goldberg MV, Getnet D, Bruno TC, Yen HR, Pyle KJ, et al. Functionally distinct LAG-3 and PD-1 subsets on activated and chronically stimulated CD8 T cells. J Immunol 2009;182:6659–69.
25. Grosso JF, Kelleher CC, Harris TJ, Maris CH, Hipkiss EL, De Marzo A, et al. LAG-3 regulates CD8+ T cell accumulation and effector function in murine self- and tumor-tolerance systems. J Clin Invest 2007;117:3383–92.
26. Keir ME, Butte MJ, Freeman GJ, Sharpe AH. PD-1 and its ligands in tolerance and immunity. Annu Rev Immunol 2008;26:677–704.
27. Brahmer JR, Drake CG, Wollner I, Powderly JD, Picus J, Sharfman WH, et al. Phase I study of single-agent anti-programmed death-1 (MDX-1106) in refractory solid tumors: safety, clinical activity, pharmacodynamics, and immunologic correlates. J Clin Oncol 2010;28:3167–75.
28. Hodi FS, O'Day SJ, McDermott DF, Weber RW, Sosman JA, Haanen JB, et al. Improved survival with ipilimumab in patients with metastatic melanoma. N Engl J Med 2010;363:711–23.
29. Workman CJ, Vignali DA. The CD4-related molecule, LAG-3 (CD223), regulates the expansion of activated T cells. Eur J Immunol 2003;33:970–9.
30. Nishimura H, Minato N, Nakano T, Honjo T. Immunological studies on PD-1 deficient mice: implication of PD-1 as a negative regulator for B cell responses. Int Immunol 1998;10:1563–72.
31. Woo SR, Li N, Bruno TC, Forbes K, Brown S, Workman C, et al. Differential subcellular localization of the regulatory T-cell protein LAG-3 and the coreceptor CD4. Eur J Immunol 2010;40:1768–77.
32. Kocak E, Lute K, Chang X, May KF Jr, Exten KR, Zhang H, et al. Combination therapy with anti-CTL antigen-4 and anti-4–1BB antibodies enhances cancer immunity and reduces autoimmunity. Cancer Res 2006;66:7276–84.
33. Collison LW, Chaturvedi V, Henderson AL, Giacomin PR, Guy C, Bankoti J, et al. IL-35-mediated induction of a potent regulatory T cell population. Nat Immunol 2010;11:1093–101.
34. Turk MJ, Guevara-Patino JA, Rizzuto GA, Engelhorn ME, Sakaguchi S, Houghton AN. Concomitant tumor immunity to a poorly immunogenic melanoma is prevented by regulatory T cells. J Exp Med 2004;200:771–82.

Downloaded from cancerres.aacrjournals.org on July 6, 2012
Copyright © 2012 American Association for Cancer Research

Published OnlineFirst December 20, 2011; DOI:10.1158/0008-5472.CAN-11-1620

35. Park D, Lapteva N, Seethammagari M, Slawin KM, Spencer DM. An essential role for Akt1 in dendritic cell function and tumor immunotherapy. Nat Biotechnol 2006;24:1581–90.
36. Li B, VanRoey M, Wang C, Chen TH, Korman A, Jooss K. Anti-programmed death-1 synergizes with granulocyte macrophage colony-stimulating factor–secreting tumor cell immunotherapy providing therapeutic benefit to mice with established tumors. Clin Cancer Res 2009;15:1623–34.
37. Workman CJ, Rice DS, Dugger KJ, Kurschner C, Vignali DA. Phenotypic analysis of the murine CD4-related glycoprotein, CD223 (LAG-3). Eur J Immunol 2002;32:2255–63.
38. Noya O, Alarcon de Noya B. The multiple antigen blot assay (MABA): a simple immunoenzymatic technique for simultaneous screening of multiple antigens. Immunol Lett 1998;63:53–6.
39. Goldberg MV, Maris CH, Hipkiss EL, Flies AS, Zhen L, Tuder RM, et al. Role of PD-1 and its ligand, B7-H1, in early fate decisions of CD8 T cells. Blood 2007;110:186–92.
40. Paradis TJ, Floyd E, Burkwit J, Cole SH, Brunson B, Elliott E, et al. The anti-tumor activity of anti-CTLA-4 is mediated through its induction of IFN gamma. Cancer Immunol Immunother 2001;50:125–33.
41. Leach DR, Krummel MF, Allison JP. Enhancement of antitumor immunity by CTLA-4 blockade. Science 1996;271:1734–6.
42. Rosenberg SA, Spiess P, Lafreniere R. A new approach to the adoptive immunotherapy of cancer with tumor-infiltrating lymphocytes. Science 1986;233:1318–21.
43. Adler AJ, Marsh DW, Yochum GS, Guzzo JL, Nigam A, Nelson WG, et al. $CD4^+$ T cell tolerance to parenchymal self-antigens requires presentation by bone marrow-derived antigen-presenting cells. J Exp Med 1998;187:1555–64.
44. Iwai Y, Terawaki S, Honjo T. PD-1 blockade inhibits hematogenous spread of poorly immunogenic tumor cells by enhanced recruitment of effector T cells. Int Immunol 2005;17:133–44.
45. Workman CJ, Wang Y, El Kasmi KC, Pardoll DM, Murray PJ, Drake CG, et al. LAG-3 regulates plasmacytoid dendritic cell homeostasis. J Immunol 2009;182:1885–91.
46. Zhang P, Cote AL, de Vries VC, Usherwood EJ, Turk MJ. Induction of postsurgical tumor immunity and T-cell memory by a poorly immunogenic tumor. Cancer Res 2007;67:6468–76.
47. Okazaki T, Okazaki IM, Wang J, Sugiura D, Nakaki F, Yoshida T, et al. PD-1 and LAG-3 inhibitory co-receptors act synergistically to prevent autoimmunity in mice. J Exp Med 2011;208:395–407.
48. Bettini M, Szymczak-Workman AL, Forbes K, Castellaw AH, Selby M, Pan X, et al. Cutting edge: accelerated autoimmune diabetes in the absence of LAG-3. J Immunol 2011;187:3493–8.
49. Brenner GJ, Cohen N, Moynihan JA. Similar immune response to nonlethal infection with herpes simplex virus-1 in sensitive (BALB/c) and resistant (C57BL/6) strains of mice. Cell Immunol 1994;157:510–24.
50. Niewiesk S, Brinckmann U, Bankamp B, Sirak S, Liebert UG, ter Meulen V. Susceptibility to measles virus-induced encephalitis in mice correlates with impaired antigen presentation to cytotoxic T lymphocytes. J Virol 1993;67:75–81.

Downloaded from cancerres.aacrjournals.org on July 6, 2012
Copyright © 2012 American Association for Cancer Research